Integrability, multiple-solitons, breathers and lumps for a new (3+1)-dimensional Kadomtsev–Petviashvili equation

Yu-Lan Ma[a], Abdul-Majid Wazwaz[b], Bang-Qing Li[*,c,d]

[a]*School of Mathematics and Statistics, Beijing Technology and Business University, Beijing, 100048, PR China*
[b]*Department Mathematics, Saint Xavier University, Chicago, IL 60655 USA*
[c]*Academy of Systems Science, Beijing Technology and Business University, Beijing, 100048, PR China*
[d]*School of Computer, Beijing Technology and Business University, Beijing, 100048, PR China*

Abstract

In this paper, a new (3+1)-dimensional integrable Kadomtsev–Petviashvili equation is developed. Its integrability is verified by the Painlevé analysis. The bilinear form, multiple-soliton, breather and lump solutions are obtained via using the Hirota bilinear method. Furthermore, the abundant dynamical behaviors for these solutions are discovered. It is interesting that there are splitting and fusing phenomena when the lumps interact.

Key words: new (3+1)-dimensional Kadomtsev–Petviashvili equation; integrability; bilinear method; soliton; breather; lump

1. Introduction

As we know, nonlinear evolution equations have exerted considerable influence promoting the progress of science and technology. The Kadomtsev–Petviashvili (KP) equation is a well-known nonlinear model which was developed to describe long wave propagation of small amplitude propagating in plasma physics under the effect of long transverse perturbations in dispersion fluids [1]. Since then, this model has been thoroughly studied in a various fields, such as plasma physics, solid state physics, fiber optics, water engineering, oceanography, and many other areas [2–10]. Mathematically, the KP equation is used to study the stability of the celebrated Korteweg-de Vries equation in a two-dimensional setting [11–16]. The KP equation can also depict weakly two-dimensional dust acoustic waves [17], weakly nonlinear quasi-unidirectional waves [18], shallow water waves with weakly nonlinear restoring forces [19, 20]. Besides, it is integrable in the sense it exhibits multiple solitons solutions and infinite conservation laws [21, 22].

Recently, the great interest on the KP equation has led to the construction and the study of many extensions to the KP equation [23–29]. These new extended models propelled greatly the research that directly resulted in many promising findings and gave an insight into some novel physical features of scientific and engineering applications. Moreover, lump solutions, and interaction solutions between

*Corresponding author
Email addresses: `mayl@th.btbu.edu.cn` (Yu-Lan Ma), `wazwaz@sxu.edu` (Abdul-Majid Wazwaz), `libq@th.btbu.edu.cn` (Bang-Qing Li)

lumps and solitons, have attracted a great amount of attentions aiming to make more progress in solitary waves theory.

Lump solutions, sometimes also called rational function solutions or rogue wave solutions, have been widely studied by researchers for their significant features in physics and many other nonlinear fields, such as, oceanography, fiber optics, water waves, and biophysics. Lumps are different from the solitons because of its locality with high amplitude and fast attenuation [5, 30–35].

The standard Kadomtsev–Petviashvili (KP) equation reads [20–22]

$$(u_t + +6uu_x + u_{xxx})_x + u_{yy} = 0, \tag{1}$$

which admits weakly dispersive waves, with quadratic nonlinearity term $(uu_x)_x$ and a weak dispersion term u_{xxxx}.

Very recently, an extended KP (eKP) equation was proposed [23]

$$(u_t + 6uu_x + u_{xxx})_x - u_{yy} + \lambda u_{tt} + \mu u_{ty} = 0, \tag{2}$$

where λu_{tt} and μu_{ty} are added to the standard KP equation (1), $u = u(x, y, t)$ is a differentiable function and λ and μ are non-zero constants. This equation can model the surface waves and internal waves in straits or channels. Moreover, although the eKP equation (2) is not integrable, the multiple-soliton solutions were computed analytically. Furthermore, mixed solutions consisting of first-order breathers and solitons were also derived [25].

In the previous work, we in Ref. [36] developed a new extension to the standard KP equation (1), given in the form

$$(u_t + 6uu_x + u_{xxx})_x - u_{yy} + \lambda u_{tt} + \mu u_{ty} + \nu u_{xt} = 0, \tag{3}$$

where an additional term, namely νu_{xt} is added to Eq. (2). This new equation can describe more dispersion effect in a standard KP system than the eKP equation (2). In Ref. [36], we showed that these terms will preserve the integrability of the standard KP equation. In addition, multiple soliton solutions, lump, breather and interaction solutions were analytically derived. For the ease of reference, henceforth we will quote Eq. (3) as the (2+1)-dimensional Ma–Wazwaz–Li (MWL) equation.

In this article, we first develop a new (3+1)-dimensional KP model based on the MWL equations (3). Then, the Painlevé integrability, multiple-soliton, breather and lump solutions will be formally derived for this new equation.

2. Formulation of a new (3+1)-dimensional KP equation

To formulate a new (3+1)-dimensional integrable KP equation, we will use the sense we used in our earlier work [36], where we add a new term γu_{xz} to the MWL equation (3). In view of this, we present

$$(u_t + 6uu_x + u_{xxx})_x - u_{yy} + \lambda u_{tt}u_{tt} + \mu u_{ty} + \nu u_{xt} + \gamma u_{xz} = 0, \tag{4}$$

where $u = u(x, y, z, t)$ is a differentiable function with respect to the spatial variable x, y, z and the temporal variable t; and λ, μ, ν and γ are non-zero arbitrary parameters. It is obvious that this equation involves four more terms, of second-order derivatives, added to the standard KP (1) equation. Eq. (4) also portraits a new dispersion effect with respect to the variables x with z, by comparing Eq. (3). As a result, the dimension is extended to (3+1) case. It is more meaningful and useful than the standard KP equation (1), eKP equation (2) and MWL equation (3) in applications. In this work, we will illustrate this new equation possesses novel feature that the MWL equation (3) does not have.

We plan in this article to employ the Painlevé test to show that the equation (4) possesses the integrability, for specific values of the parameters λ, μ, ν and γ, provided upon using the compatibility conditions. Hence it is integrable. Most importantly, unlike the KP dispersion relations, we will show that the phase shifts of this new equation gives distinct shifts that differ from the standard KP equation phase shifts. As will be shown later, the integrability of this equation permits us to derive multiple soliton, breather, and lump solutions for the non-zero parameters λ, μ, ν and γ.

3. Painlevé Analysis to Eq. (4)

The complete integrability of nonlinear evolution equations has been an important feature in nonlinear solitary wave theory. There are many significant properties, such as Lax pair, Hamiltonian structure, infinitely many symmetries and infinite conservation laws, that can characterize the integrability of nonlinear evolution equations. To emphasize the integrability of Eq. (4), we follow the Painlevé analysis method presented in [21, 37, 38] and the some of the references therein. We get a characteristic equation for resonances at $k = -1, 4, 5$, and 6. We also find explicit expressions for u_1, u_2, u_3, and we found that u_4, u_5, u_6 turn out to be arbitrary functions, provided that the compatibility conditions, for $k = 4, 5, 6$, are satisfied for $\lambda = -\frac{\alpha^2}{4}, \mu = \alpha$, and $\nu = \beta$, where α and β are non-zero constants, and γ is left free parameter. In view of this, the (3+1)-dimensional KP equation (4) takes the form

$$(u_t + 6uu_x + u_{xxx})_x - u_{yy} - \frac{\alpha^2}{4}u_{tt} + \alpha u_{ty} + \beta u_{xt} + \gamma u_{xz} = 0. \tag{5}$$

4. Bilinear form and general solution of Eq. (5)

First of all, it is necessary to construct the bilinear form of Eq. (5) according to the Hirota bilinear theory [39, 40]. By introducing a transformation as

$$u = 2(\ln f)_{xx}, \tag{6}$$

where f is an auxiliary function to be determined later, we can get the following bilinear form of Eq. (5)

$$\left(D_x^4 + (\beta+1)\, D_t D_x + \alpha D_t D_y + \gamma D_x D_z - D_y^2 - \frac{\alpha^2}{4} D_t^2\right)(f \cdot f) = 0, \tag{7}$$

where D is a bilinear operator whose definition can be found in the existing literatures such as Refs. [41–43]

From (6), we give the generalized solution of Eq. (5)

$$u = 2\frac{ff_{xx} - f_x^2}{f^2}. \tag{8}$$

To construct the high-order solutions, we introduce a series of travelling transformations

$$\xi_i = k_i\left(x + s_i y + r_i z + w_i t\right) + \xi_{i0}, \tag{9}$$

where k_i, s_i, r_i, w_i and ξ_{i0} are non-zero constants, and $s_i = k_i$, $r_i = \frac{w_i}{\gamma}\left(\frac{\alpha^2}{4}w_i - \alpha s_i - (\beta+1)\right)$, $i \in \{1, 2, 3, \cdots, n\}$, and n is a positive integer.

5. Soliton, breather and their interaction solutions

In this section, we will seek for the exponential function solution of Eq. (5). Those solution can generate multiple-solitons and multiple-breather, even mixed soliton and breather.

5.1. The first-order exponential function solution

Lets start from a simple exponential function. Taking the auxiliary function f in the bilinear equation (7) as

$$f = f_1 = 1 + e^{\xi_1}. \tag{10}$$

It is easy to get

$$f_x = f_{1x} = k_1 e^{\xi_1}, \tag{11}$$

$$f_{xx} = k_1^2 e^{\xi_1}. \tag{12}$$

The substitution of (10), (11) and (12) into (8) will generate the first-order exponential function solution that has a bright soliton.

The profile of the solution (8) with the auxiliary function (10) exhibits bright single-soliton under all the six different coordinates. The graphs for the single-soliton are shown in Fig. 1.

5.2. The second-order exponential function solution

For the second auxiliary function, we take

$$f = f_2 = 1 + e^{\xi_1} + e^{\xi_2} + a_{12}e^{\xi_1+\xi_2}, \tag{13}$$

where a_{12} is the dispersion coefficient to be determined later. Substituting (13) into the bilinear form (7) will reach

$$a_{12} = \frac{16(k_1-k_2)^2 + \alpha\left(w_1-w_2\right)\left[\alpha\left(w_1-w_2\right) - 4\left(k_1-k_2\right)\right]}{16\left(k_1^2+k_1k_2+k_2^2\right) + \alpha\left(w_1-w_2\right)\left[\alpha\left(w_1-w_2\right) - 4\left(k_1-k_2\right)\right]}. \tag{14}$$

Further, we can verify the following proposition.

Proposition 1. For the auxiliary function composing of three exponential functions

$$f = 1 + e^{\xi_i} + e^{\xi_j} + a_{ij} e^{\xi_i + \xi_j}, \tag{15}$$

the dispersion coefficient a_{ij} satisfies the relationship

$$a_{ij} = \frac{16(k_i - k_j)^2 + \alpha (w_i - w_j) \left[\alpha (w_i - w_j) - 4 (k_i - k_j)\right]}{16 \left(k_i^2 + k_i k_j + k_j^2\right) + \alpha (w_i - w_j) \left[\alpha (w_i - w_j) - 4 (k_i - k_j)\right]}, 1 \le i < j \le n. \tag{16}$$

Through computation, it yields

$$f_x = f_{2x} = k_1 e^{\xi_1} + k_2 e^{\xi_2} + (k_1 + k_2)\, a_{12} e^{\xi_1 + \xi_2}, \tag{17}$$

$$f_{xx} = f_{2xx} = k_1^2 e^{\xi_1} + k_2^2 e^{\xi_2} + (k_1 + k_2)^2 a_{12} e^{\xi_1 + \xi_2}. \tag{18}$$

The substitution of (13), (17), (18) and (13) into (8), can derive the second-order exponential function solution of Eq. (5), which may appear as two-solitons or single-breather.

Because of the inherent nonlinear properties of the equation, the interaction between waves can emerge interesting and important characteristics. As the two-solitons interact, there exist engrossing dynamics. Firstly, all the interactions between the solitons are elastic, namely, the spreading speeds and amplitudes of these solitons will remain unchanged before and after the collisions. Secondly, their phases may shift during the interaction process. Besides, there may exist the amplitude resonances when the solitons collide. Fig. 2 demonstrates three typical examples: (i) Amplitude superposition resonance (see Fig. 2(a)); (ii) Amplitude collapse resonance (see Fig. 2(b)); (iii) Collision without contact and without amplitude variant (see Fig. 2(c)).

Especially, as the dispersion coefficients k_1 and k_2, w_1 and w_2 are taken as a pair of conjugate complex numbers, namely, $k_2 = k_1^*$, $w_1 = w_1^*$, here * stands for the conjugate complex number of the indicated constants, the solution (8) with (13) appears as single-breather (see Fig. 3).

Remark 1: For the sake to save space, we just give the graphs of the solution (8) with (13) under the $x - z - u$ with $y = t = 0$. In fact, the graphs of the solution under other five types of coordinates are like this case. For the next higher-order solutions, we also do the same thing.

5.3. The third-order exponential function solution

In order to construct the third-order solution, it is sensible to take the auxiliary function f as

$$f = f_3 = 1 + \sum_{i=1}^{3} e^{\xi_i} + \sum_{1 \le i < j \le 3} a_{ij} e^{\xi_i + \xi_j} + a_{123} e^{\sum_{i=1}^{3} \xi_i}, \tag{19}$$

where $a_{ij}, 1 \le i < j \le 3$ satisfies the relationship expression (16). More, the dispersion coefficient a_{123} can be verifies to satisfy the following constrain

$$a_{123} = a_{12} a_{13} a_{23}. \tag{20}$$

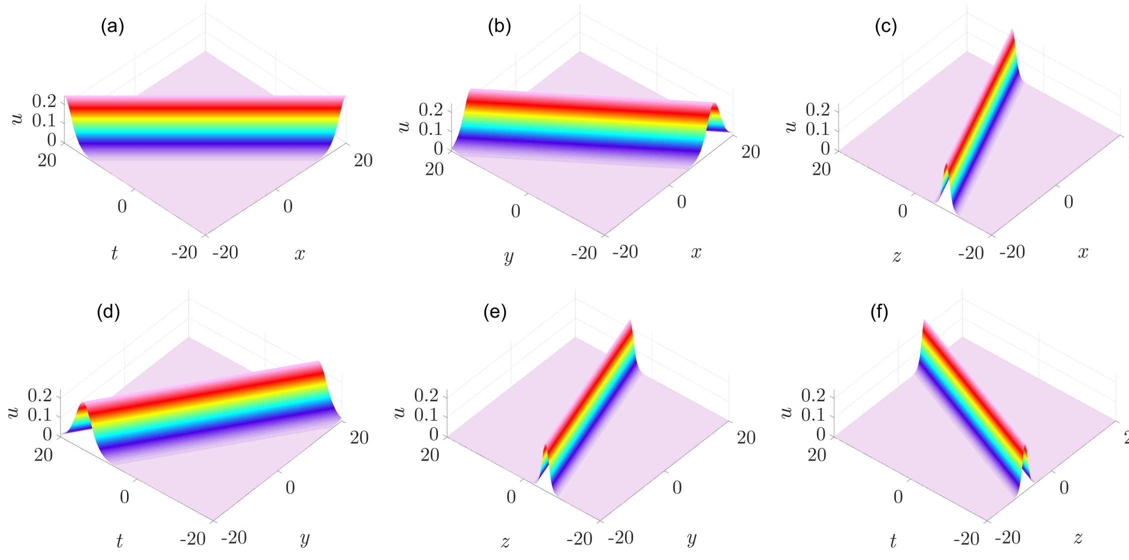

Fig. 1: The single-soliton. The plots are given by the solution (8) with the auxiliary function (10), and the settings: $\alpha = 1, \beta = 1, \gamma = 1, \xi_{10} = 0$, $k_1 = 0.7, w_1 = 1$. (a) $y = z = 0$ under $x - t - u$ coordinate; (b) $z = t = 0$ under $x - y - u$ coordinate; (c) $y = t = 0$ under $x - z - u$ coordinate; (d) $x = z = 0$ under $y - t - u$ coordinate; (e) $x = t = 0$ under $y - z - u$ coordinate; (f) $x = y = 0$ under $z - t - u$ coordinate.

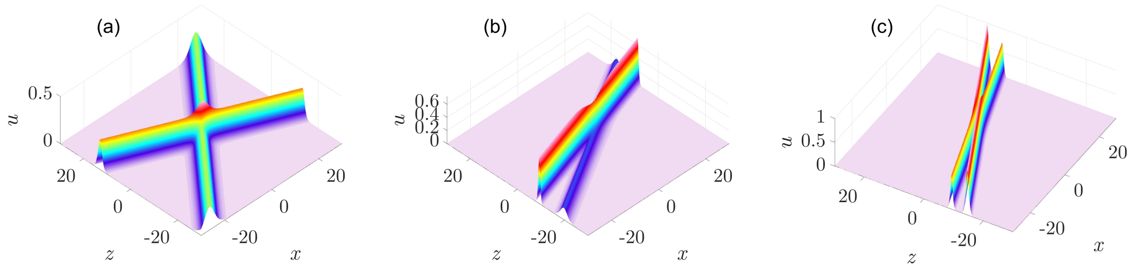

Fig. 2: The two-solitons. The plots are given by the solution (8) with the auxiliary function (13) under the $x - z$-coordinate, and the settings: $y = 0, t = 0, \alpha = 1, \beta = 1, \gamma = 1, \xi_{10} = \xi_{20} = 0$, and (a) $k_1 = -0.7, k_2 = 0.8, w_1 = 0.8, w_2 = -0.75$, (a) $k_1 = 1.2, k_2 = 0.6, w_1 = 1.1, w_2 = 0.7$, (a) $k_1 = 1.2, k_2 = 1.4, w_1 = 1.1, w_2 = 0.7$.

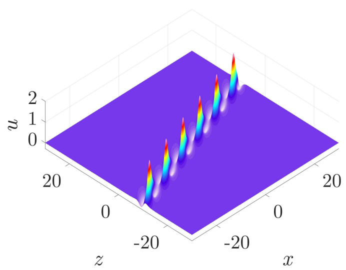

Fig. 3: The single-breather. The plot is given by the solution (8) with the auxiliary function (13) under the $x - z$-coordinate, and the settings: $y = 0, t = 0, \alpha = 1, \beta = 1, \gamma = 1, \xi_{10} = \xi_{20} = 0$, and $k_1 = 0.4 + 0.8I, w_1 = 0.3 - 0.5I, I = \sqrt{-1}$, $k_2 = k_1^*, w_2 = w_1^*$.

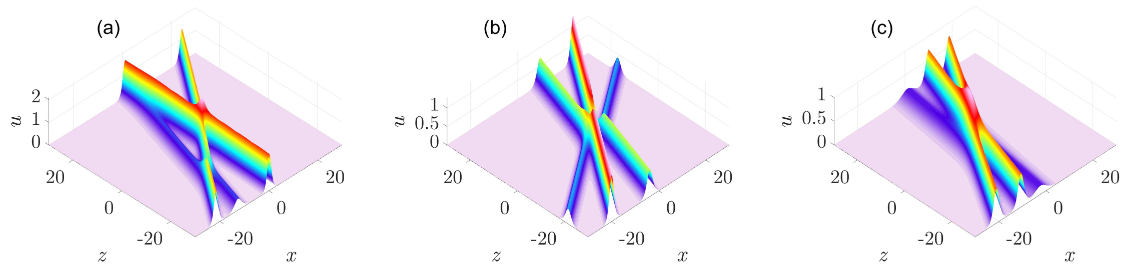

Fig. 4: The three-solitons. The plots are given by the solution (8) with the auxiliary function (19), and the settings: $y = 0, t = 0, \alpha = 1, \beta = 1, \gamma = 1,\ w_1 = 0.5, w_2 = 0.1, w_3 = 0.2$, and (a) $\xi_{10} = 0, \xi_{20} = 5, \xi_{30} = -2, k_1 = -1.8, k_2 = 1, k_3 = 1.7$, (b) $\xi_{10} = \xi_{20} = \xi_{30} = 0, k_1 = 0.9, k_2 = 1.2, k_3 = 1.6$, (c) $\xi_{10} = \xi_{20} = \xi_{30} = 0, k_1 = -1.2, k_2 = -0.6, k_3 = 1.2$.

Furthermore, we naturally think to extend the above third-order auxiliary function f_3 and its dispersion coefficient a_{123} to the general form. Therefore, we give the following proposition.

Proposition 2. For the general third-order auxiliary function

$$f = 1 + e^{\xi_i} + e^{\xi_j} + e^{\xi_l} + a_{ij}e^{\xi_i+\xi_j} + a_{il}e^{\xi_i+\xi_l} + a_{jl}e^{\xi_j+\xi_l} + a_{ijl}e^{e^{\xi_i}+e^{\xi_j}+e^{\xi_l}}, \tag{21}$$

where $1 \le i < j < l \le n$, the third-order dispersion coefficient a_{ijl} satisfies

$$a_{ijl} = a_{ij}a_{il}a_{jl}. \tag{22}$$

From (19), ones can get

$$f_x = f_{3x} = \sum_{i=1}^{3} k_i e^{\xi_i} + \sum_{1\le i<j\le 3} (k_i + k_j)\, a_{ij}e^{\xi_i+\xi_j} + \left(\sum_{i=1}^{3} k_i\right) a_{123}e^{\sum_{i=1}^{3}\xi_i}, \tag{23}$$

$$f_{xx} = f_{3xx} = \sum_{i=1}^{3} k_i^2 e^{\xi_i} + \sum_{1\le i<j\le 3} (k_i + k_j)^2 a_{ij}e^{\xi_i+\xi_j} + \left(\sum_{i=1}^{3} k_i\right)^2 a_{123}e^{\sum_{i=1}^{3}\xi_i}. \tag{24}$$

Thus, the three-order solution can be obtained by substituting of (19), (23) and (24) into (8).

If all the dispersion coefficients k_1, k_2, k_3, w_1, w_2 and w_3 are set as real constants, the three-order solution exhibits as the three-solitons.

As the tree-solitons interact, there exist still amplitude resonant at the collision points displayed in Fig. 4. In addition, the three-solitons possess certain new characteristics, for example, triangle-like intersection as the constants ξ_{10}, ξ_{20} and ξ_{30} in the expression (9) are taken at different values (see Fig. 4(a)).

Especially, as the two of the dispersion coefficients k_i $(i = 1, 2, 3)$ and the two of w_i $(i = 1, 2, 3)$ are taken as a pair of conjugate complex numbers, the solution (8) with (19) displays the mixed single-solitons and single-breather (see Fig. 5).

5.4. The fourth-order exponential function solution

For the fourth-order auxiliary function f_4, we choose

$$f = f_4 = 1 + \sum_{i=1}^{4} e^{\xi_i} + \sum_{1\le i<j\le 4} a_{ij}e^{\xi_i+\xi_j} + \sum_{1\le i<j<l\le 4} a_{ijl}e^{\xi_i+\xi_j+\xi_l} + a_{1234}e^{\sum_{i=1}^{4}\xi_i}, \tag{25}$$

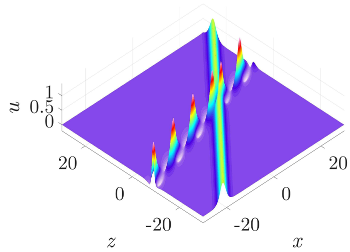

Fig. 5: The mixed single-soliton and single-breather. The plots are given by the solution (8) with the auxiliary function (19), and the settings: $y = 0, t = 0, \alpha = 1, \beta = 1, \gamma = 1, \xi_{10} = \xi_{20} = \xi_{30} = 0,\ k_1 = 0.4 + 0.7I, k_2 = k_1^*, k_3 = 1.2, w_1 = 0.4 - 0.6I, w_2 = w_1^*, w_3 = 0.3$.

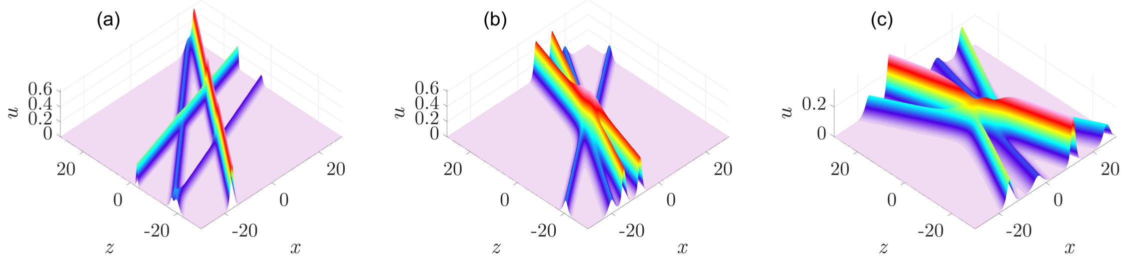

Fig. 6: The four-solitons. The plots are given by the solution (8) with the auxiliary function (25), and the settings: $y = 0, t = 0, \alpha = 1, \beta = 1, \gamma = 1$, and (a) $\xi_{10} = -5, \xi_{20} = -8, \xi_{30} = 5, \xi_{40} = 15, k_1 = -0.6, k_2 = 0.5, k_3 = -1.1, k_4 = 0.8, w1 = 1, w_2 = 1.2, w_3 = 1.3, w_4 = 1.4$, (b) $\xi_{10} = \xi_{20} = \xi_{30} = \xi_{40} = 0, k_1 = -0.6, k_2 = 0.6, k_3 = -1, k_4 = 1,\ w1 = 1, w_2 = 1.2, w_3 = 1.3, w_4 = 1.4$, (c) $\xi_{10} = \xi_{20} = \xi_{30} = \xi_{40} = 0, k_1 = 0.4, k_2 = 0.6, k_3 = -1, k_4 = 1,\ w1 = 0.1, w_2 = 1.2, w_3 = -0.2, w_4 = -0.1$.

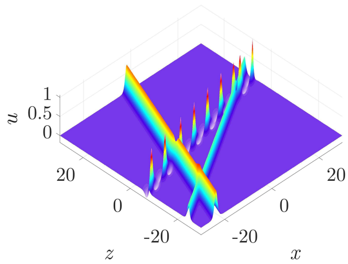

Fig. 7: The mixed two-solitons and single-breather. The plots are given by the solution (8) with the auxiliary function (25), and the settings: $y = 0, t = 0, \alpha = 1, \beta = 1, \gamma = 1$, $\xi_{10} = \xi_{20} = 0, \xi_{30} = -10, \xi_{40} = -16$, $k_1 = 0.25 + 0.5I, k_2 = k_1^*, k_3 = 0.9, k_4 = -1.2$, $w1 = -0.4 - 0.7I, w_2 = w_2^*, w_3 = 0.6, w_4 = 0.5$, where $I = \sqrt{-1}$.

where a_{ij} and a_{ijl} satisfy the expression (16) and (22), respectively.

By calculation, we can find out that the forth-order dispersion coefficient a_{1234} must match the relationship

$$a_{1234} = a_{12}a_{13}a_{14}a_{23}a_{24}a_{34}. \tag{26}$$

From (25), we are able to calculate out

$$f_x = f_{4x} = \sum_{i=1}^{4} k_i e^{\xi_i} + \sum_{1\le i<j\le 4} (k_i + k_j)\, a_{ij} e^{\xi_i+\xi_j} + \sum_{1\le i<j<l\le 4} (k_i + k_j + k_l)\, a_{ijl} e^{\xi_i+\xi_j+\xi_l} + \left(\sum_{i=1}^{4} k_i\right) a_{1234} e^{\sum_{i=1}^{4}\xi_i}, \tag{27}$$

$$f_{xx} = f_{4xx} = \sum_{i=1}^{4} k_i^2 e^{\xi_i} + \sum_{1\le i<j\le 4} (k_i + k_j)^2 a_{ij} e^{\xi_i+\xi_j} + \sum_{1\le i<j<l\le 4} (k_i + k_j + k_l)^2 a_{ijl} e^{\xi_i+\xi_j+\xi_l} + \left(\sum_{i=1}^{4} k_i\right)^2 a_{1234} e^{\sum_{i=1}^{4}\xi_i}. \tag{28}$$

By substituting (25), (27) and (28) into (8), the fourth-order solution can be attained for Eq. (5).

There are three types of combinations for the fourth-order solution: (i) The four-solitons as k_i and w_i $(i = 1, 2, 3, 4)$ taken as real numbers (see Fig. 6); (ii) The mixed two-solitons and single-breather as one pair of k_i $(i = 1, 2, 3, 4)$ and one pair of w_i $(i = 1, 2, 3, 4)$ are taken complex numbers, and the others as real numbers Fig. 7); (iii) The two-breathers as k_i $(i = 1, 2, 3, 4)$ taken as two pairs of conjugate complex numbers Fig. 8).

Remark 2: Following the above schemes, the higher-order exponential function solutions $(n > 4)$ of Eq. (5) can be acquire. However, the computation complexity will increase exponentially as the order increases.

6. Lump solutions

The lump solutions can be expressed by rational or semi-rational functions. So, to construct the lump solution of Eq. (5), finding suitable rational auxiliary function f is critical. As the first step, we

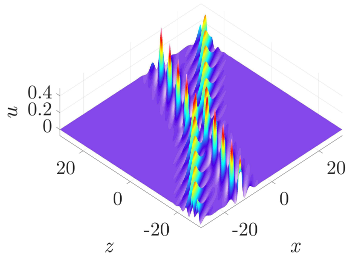

Fig. 8: The two-breathers. The plots are given by the solution (8) with the auxiliary function (25), and the settings: $y = 0, t = 0, \alpha = 1, \beta = 1, \gamma = 1,\ \xi_{10} = \xi_{20} = \xi_{30} = \xi_{40} = 0,\ k_1 = 0.3 + 0.6I, k_2 = k_1^*, k_3 = 0.25 + 0.5I, k_4 = k_3^*$, $w1 = w_2 = 0.5, w_3 = w_4 = 1$, where $I = \sqrt{-1}$.

now introduce a new series of transformations as

$$\theta_i = x + a_i y + b_i z + c_i t + \theta_{i0}, \tag{29}$$

where a_i, b_i, c_i and θ_{i0} are non-zero constants, and $b_i = \frac{a_i^2 - c_i\left(\beta+1+\alpha a_i - \frac{\alpha^2}{4}c_i\right)}{\gamma}$, $i \in \{1, 2, 3, \cdots, n\}$, n is a positive integer.

6.1. The single-lump solution

For the single-lump solution, we construct the auxiliary function f as

$$f = f_{1lump} = \theta_1\theta_2 + h_{12}, \tag{30}$$

where θ_1 and θ_2 are given by (29) as $i = 1$ and 2, respectively, h_{12} is an undetermined dispersion coefficient.

By putting (30) into the bilinear expression (7), we can derive

$$h_{12} = \frac{-12}{(\beta+1)(c_1+c_2) + \alpha(a_1c_2 + a_2c_1) - 2a_1a_2 + \gamma(b_1+b_2) - \frac{\alpha^2}{2}c_1c_2}. \tag{31}$$

It is easy to get

$$f_x = (f_{1lump})_x = \theta_1 + \theta_2, \tag{32}$$

$$f_{xx} = (f_{1lump})_{xx} = 2. \tag{33}$$

By substituting (30), (32) and (33) into (8), the single-lump solution is obtained.

Subsequently, we are able to verify following proposition.

Proposition 3. For the auxiliary function

$$f = f_{1lump} = \theta_l\theta_k + h_{lk}, 1 < l < k \leq n, \tag{34}$$

where θ_l and θ_k are given by (29) with $i = l, k$, the dispersion coefficient h_{lk} satisfies

$$h_{lk} = \frac{-12}{(\beta+1)(c_l+c_k) + \alpha(a_lc_k + a_kc_l) - 2a_la_k + \gamma(b_l+b_k) - \frac{\alpha^2}{2}c_lc_k}. \tag{35}$$

The Fig. 9 shows the profile of the single-lump solution (8) with (30) in all the six coordinates, which is localized to all the variables with one peak and two troughs.

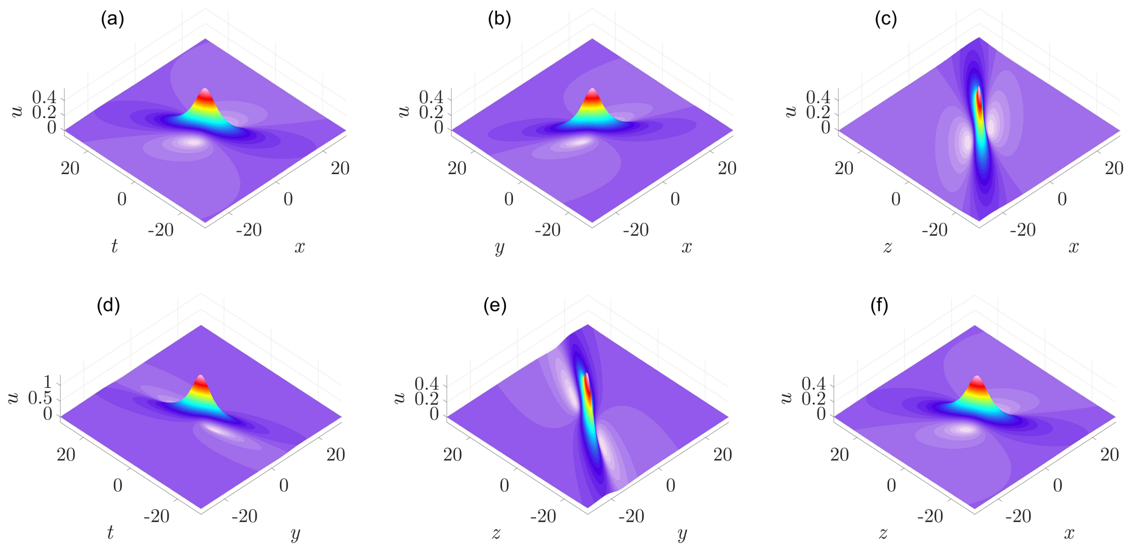

Fig. 9: The single-lump. The plots are given by the solution (8) with the auxiliary function (36), and the settings: $\alpha = 1, \beta = 1, \gamma = 1, \theta_{10} = \theta_{20} = 0,\ a_1 = 1 - I, a_2 = a_1^*, c_1 = 0.5 - 0.7I, c_2 = c_1^*$, where $I = \sqrt{-1}$, (a) $y = z = 0$ under $x - t - u$ coordinate; (b) $z = t = 0$ under $x - y - u$ coordinate; (c) $y = t = 0$ under $x - z - u$ coordinate; (d) $x = z = 0$ under $y - t - u$ coordinate; (e) $x = t = 0$ under $y - z - u$ coordinate; (f) $x = y = 0$ under $z - t - u$ coordinate.

6.2. The two-lump solution

In order to obtain the two-lump solution, we choose the auxiliary function f as

$$f = f_{2lump} = \prod_{i=1}^{4} \theta_i + h_{34}\theta_1\theta_2 + h_{24}\theta_1\theta_3 + h_{23}\theta_1\theta_4 + h_{14}\theta_2\theta_3 + h_{13}\theta_2\theta_4 + h_{12}\theta_3\theta_4 + h_{1234}, \tag{36}$$

where θ_i is given by (29) with $i = 1, 2, 3, 4$, h_{lk} $(1 \leq l < k \leq 4)$ is given by (35), h_{1234} is the undetermined second-order coefficient.

Through the substitution of (36) into (7), we find out h_{1234} have to satisfy

$$h_{1234} = h_{12}h_{34} + h_{13}h_{24} + h_{14}h_{23}. \tag{37}$$

Then, we can attain

$$\begin{aligned} f_x = (f_{2lump})_x &= \theta_2\theta_3\theta_4 + \theta_1\left(\theta_2\theta_3 + \theta_2\theta_4 + \theta_3\theta_4\right) + \left(h_{23} + h_{24} + h_{34}\right)\theta_1 \\ &+ \left(h_{13} + h_{14} + h_{34}\right)\theta_2 + \left(h_{12} + h_{14} + h_{24}\right)\theta_3 + \left(h_{12} + h_{13} + h_{23}\right)\theta_4, \end{aligned} \tag{38}$$

$$\begin{aligned} f_{xx} = (f_{2lump})_{xx} &= 2\left[\theta_1\left(\theta_2 + \theta_3 + \theta_4\right) + \theta_2\left(\theta_3 + \theta_4\right) + \theta_3\theta_4\right. \\ &\left.+ h_{12} + h_{13} + h_{14} + h_{23} + h_{24} + h_{34}\right]. \end{aligned} \tag{39}$$

The two-lump solution can be obtained by substituting (36), (38) and (39) into (8).

We discover there are two types of interaction characteristics between two-lumps by taking the dispersion coefficients at the proper values: (i) Splitting behavior. The interaction between the two-lumps start from two completely separated lumps (see Fig. 10(a)). Then, the two lumps are evolving into a

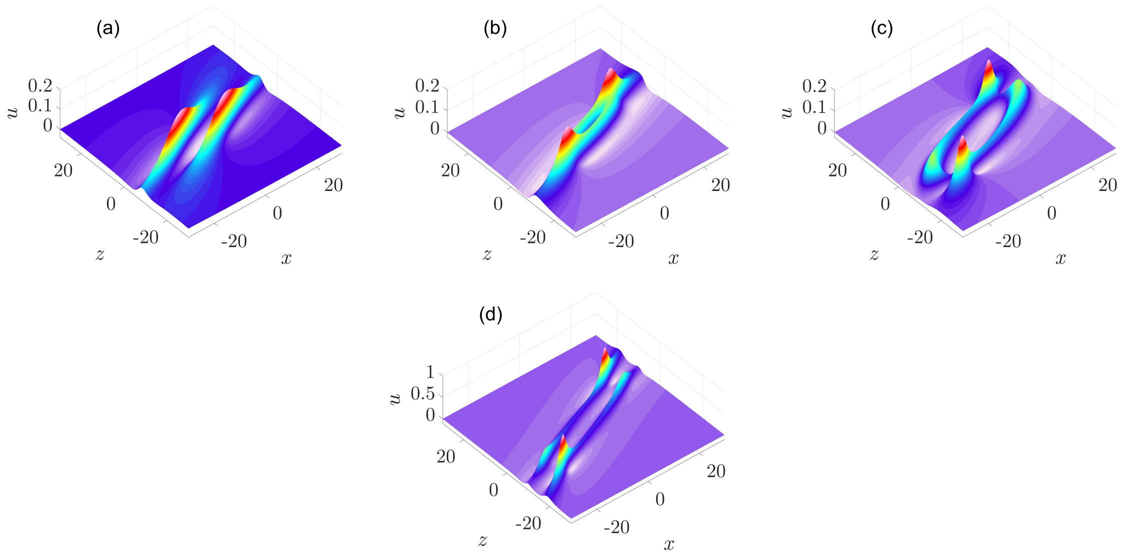

Fig. 10: The splitting of the two-lumps. The plots are given by the solution (8) with the auxiliary function (36), and the settings: $y=0, t=0, \alpha=1, \beta=1, \gamma=1, \theta_{10}=\theta_{20}=\theta_{30}=\theta_{40}=0$, (a) $a_1=0.3-0.2I, a_2=a_1^*, a_3=0.4+0.8I, a_4=a_3^*, c_1=0.5+0.5I, c_2=c_1^*, c3=1.3+0.5I, c_4=c_3^*$, (b) $a_1=0.3-0.6I, a_2=a_1^*, a_3=0.4+0.8I, a_4=a_3^*, c_1=0.5+0.5I, c_2=c_1^*, c3=1.3+0.5I, c_4=c_3^*$, (c) $a_1=0.3-0.12I, a_2=a_1^*, a_3=0.4+0.8I, a_4=a_3^*, c_1=0.5+0.5I, c_2=c_1^*, c3=1.1+1I, c_4=c_3^*$, (d) $a_1=0.3-0.6I, a_2=a_1^*, a_3=0.4+0.8I, a_4=a_3^*, c_1=0.5+0.2I, c_2=c_1^*, c3=1.3+0.3I, c_4=c_3^*$, where $I=\sqrt{-1}$.

linked state (see Fig. 10(b)). Subsequently, they are gradually generating two new lumps (see Fig. 10(c) and (d)). (ii) Fusing behavior. The separated two-lumps may gradually merge into one lump. What's even more amazing is that the amplitude after the fusion is remained unchanged. The fusing process is exhibited in Fig. 11.

The results are not only greatly different the amplitude resonance effect for the multiple-solitons observed in the above section, but also different the two-lumps interaction of the (2+1)-dimensional MWL equation (3), where the two-lumps do not split and fuse under the same settings.

Remark 3: Following the above schemes, the higher-order rational function or multiple lump solutions ($n>2$) of Eq. (5) can also be attained. This is secured for the integrability of Eq. (5) confirmed in Section 3. However, the computation complexity will also increase exponentially as the order n increases.

7. Conclusions

In this work, a new (3+1)-dimensional KP equation was first proposed to portrait more dispersion effect in nonlinear science. We used the Painlevé analysis method to study the compatibility conditions to ensure the integrability. Then, its bilinear form was derived. By smart choices for the auxiliary function in the bilinear form, higher-order exponential function solutions are obtained which can exhibit multiple-solitons, multiple-breathers or their mixed forms. The rational function solutions for this equation also attained which can display lumps. This work further proved the complete integrability of the newly developed equation, as it admits the bilinear representation, and N-soliton solutions.

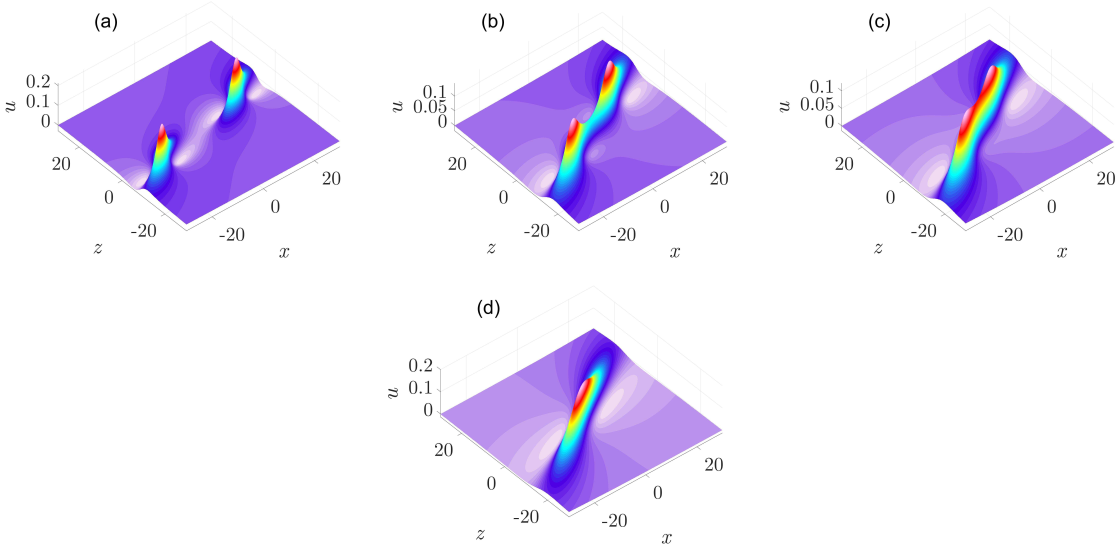

Fig. 11: The fusion of the two-lumps. The plots are given by the solution (8) with the auxiliary function (36), and the settings: $y = 0, t = 0, \alpha = 1, \beta = 1, \gamma = 1, \theta_{10} = \theta_{20} = \theta_{30} = \theta_{40} = 0$, $a_1 = 0.3 - 0.2I, a_2 = a_1^*, a_3 = 0.5 + 0.1I, a_4 = a_3^*, c_1 = 0.5 + 0.5I, c_2 = c_1^*$, and different c_3 and c_4 (a) $c3 = 0.5 + 0.9I$, (b) $c3 = 0.5 + 0.6I$, (c) $c3 = 0.5 + 0.5I$, (d) $c3 = 0.5 + 0.4I$, and $c_4 = c_3^*$, where $I = \sqrt{-1}$.

Furthermore, some interesting interaction behaviors between these waves are observed, such as elastic collision, phase transition, amplitude resonance effect.

It is very magical that the two-lumps may split into four and fuse into one. This result is also rare in the previous literatures within our best knowledge. Actually, the MWL equation (3) does not possess this novel property (also refer [36]).

We would like to think this new (3+1)-dimensional model and the research on it may be of favor on opening a new insight for future nonlinear evolution systems. The more study on other integrable properties and other exact solutions of this new integrable model is worthwhile in the future.

Compliance with ethical standards

The authors ensure the compliance with ethical standards for this work.

Conflict of interest:

The authors declare that there are no conflicts of interests with publication of this work.

References

[1] B.B. Kadomtsev, V.I. Petviashvili, On the stability of solitary waves in weakly dispersive media, Sov. Phys. Dokl., 15 (1970) 539–541.

[2] C.W. Cao, Y.T. Wu, X.G. Geng, Relation between the Kadometsev–Petviashvili equation and the confocal involutive system, J. Math. Phys. 40 (1999) 3948–3970.

[3] Y.T. Gao, B. Tian, On the non-planar dust-ion-acoustic waves in cosmic dusty plasmas with transverse perturbations, EPL 77 (2007) 15001.

[4] H. Leblond, D. Mihalache, Models of few optical cycle solitons beyond the slowly varying envelope approximation, Phys. Rep.-Rev. Sec. Phys. Lett. 523 (2013) 61–126.

[5] W.X. Ma, Lump solutions to the Kadomtsev–Petviashvili equation, Phys. Lett. A 379 (2015) 1975–1978.

[6] X.B. Wang, S.F. Tian, H. Yan, T.T. Zhang, On the solitary waves, breather waves and rogue waves to a generalized (3+1)-dimensional Kadomtsev-Petviashvili equation, Comput. Math. Appl.

[7] C.Y. Qin, S.F. Tian, X.B. Wang, T.T. Zhang, J. Li, Rogue waves, bright-dark solitons and traveling wave solutions of the (3+1)-dimensional generalized Kadomtsev-Petviashvili equation, Comput. Math. Appl 75 (2018) 4221–4231.

[8] Y.L. Ma, B.Q. Li, Rogue wave solutions, soliton and rogue wave mixed solution for a generalized (3+1)-dimensional Kadomtsev-Petviashvili equation in fluids, Mod. Phys. Lett. B 32 (2018) 1850358.

[9] W. Li, Y. Zhang, Y.P. Liu, Exact wave solutions for a (3+1)-dimensional generalized B-type Kadomtsev-Petviashvili equation, Comput. Math. Appl. 77 (2019) 3087–3101.

[10] C. Yuan, Z. Wang, X. Chen, The derivation of an isotropic model for internal waves and its application to wave generation, Ocean Model. 153 (2020) 101663.

[11] D.E. Bar, A.A. Nepomnyashchy, Stability of periodic waves generated by long-wavelength instabilities in isotropic and anisotropic systems, Physica D 132 (1999) 411–427.

[12] L. Wei, Y. He, S. Kumar, Numerical study based on an implicit fully discrete local discontinuous Galerkin method for time fractional KdV–Burgers Kuramoto equation, ZAMM J. Appl. Math. Mechan. 93 (2013) 14–28.

[13] S. Kumar, M. Tripathi, Q.P. Singh, A fractional model of Harry Dym equation and its approximate solution, Ain Shams Engineering Journal, 4 (2013) 111–115.

[14] L. Kaur, A.M. Wazwaz, Painlevé analysis and invariant solutions of generalized fifth-order nonlinear integrable equation, Nonlinear Dyn. 94 (2018) 2469–2477.

[15] X.L. Wang, L. Yu, M.R. Chen, On generalized Lax equation of the Lax triple of KP hierarchy, J. Nonlin. Math. Phys. 22 (2015) 194–203.

[16] A.M. Wazwaz, Two new integrable fourth-order nonlinear equations: multiple soliton solutions and multiple complex soliton solutions, Nonlinear Dyn. 94 (2018) 2655–2663.

[17] W.S. Duan, Weakly two-dimensional dust acoustic waves, Phys. Plasmas 8 (2001) 3583–3586.

[18] W. Ben Youssef, D. Lannes, The long wave limit for a general class of 2D quasilinear hyperbolic problems, Commun. Partial Differ. Equ. 27 (2002) 979–1020.

[19] X.H. Meng, Rational solutions in Grammian form for the (3+1)-dimensional generalized shallow water wave equation, Comput. Math. Appl. 75 (2018) 4534–4539.

[20] J.G. Liu, X.J. Yang, Y.Y. Feng, Characteristic of the algebraic traveling wave solutions for two extended (2+1)-dimensional Kadomtsev–Petviashvili equations, Mod. Phys. Lett. A 35 (2020) 2050028.

[21] A.M. Wazwaz, Kadomtsev–Petviashvili hierarchy: N-soliton solutions and distinct dispersion, Appl. Math. Lett. 52 (2016) 74–79.

[22] T. Wolf, A comparison of four approaches to the calculation of conservation laws, Eur. J. Appl. Math. 13 (2002) 129–152.

[23] S. Manukure, Y. Zhou, W.X. Ma, Lump solutions to a (2+1)-dimensional extended KP equation, Comput. Math. Appl. 75 (2018) 2414–2419.

[24] X. Guan, W.J. Liu, Q. Zhou, A. Biswas A, Some lump solutions for a generalized (3+1)-dimensional Kadomtsev–Petviashvili equation, Appl. Math. Comput., 366 (2020) 124757.

[25] J. Guo, J. He, M. Li. D. Mihalache, Exact solutions with elastic interactions for the (2 +1)-dimensional extended Kadomtsev–Petviashvili equation, Nonlinear Dyn. 101 (2020) 2413–2422.

[26] D. Wu, The direct scattering problem for the perturbed Gr(1,2)(¿ 0)Kadomtsev-Petviash-vili II solitons, Nonlinearity 33 (2020) 6729-6759

[27] N. Xiong, W.T. Li, B. Li, Weakly Coupled B-Type Kadomtsev-Petviashvili Equation: Lump and Rational Solutions, Adv. Math. Phys. 2020 (2020) 6185391.

[28] M.F. Hoque, H.O. Roshid, F.S. Alshammari, Higher-order rogue wave solutions of the Kadomtsev Petviashvili-Benjanim Bona Mahony (KP-BBM) model via the Hirota-bilinear approach, Physica Scr. 95 (2020) 115215.

[29] B. Ghanbari, H. Gunerhan, S. Momani, Exact optical solutions for the regularized long-wave Kadomtsev-Petviashvili equation, Physica Scr. 95 (2020) 105208.

[30] B.L. Guo, L.M. Ling, Q.P. Liu, Nonlinear Schrödinger equation: Generalized Darboux transformation and rogue wave solutions, Phys. Rev. E 85, (2012) 026607.

[31] B.Q. Li, Y.L. Ma, Multiple-lump waves for a (3+1)-dimensional Boiti–Leon–Manna–Pempinelli equation arising from incompressible fluid, Comput. Math. Appl. 76 (2018) 204–214.

[32] Y.L. Ma, B.Q. Li, Analytic rogue wave solutions for a generalized fourth-order Boussinesq equation in fluid mechanics, Math. Methods Appl. Sci. 42 (2019) 39–48.

[33] J.P. Yu, F.D. Wang, W.X. Ma, Y.L. Sun, C.M. Khalique, Multiple-soliton solutions and lumps of a (3+1)-dimensional generalized KP equation, Nonlinear Dyn. 95 (2019) 1687–1692.

[34] Y.L. Ma, B.Q. Li, Mixed lump and soliton solutions for a generalized (3+1)-dimensional Kadomtsev-Petviashvili equation, AIMS Mathematics, 5 (2020) 1162–1176.

[35] B.Q. Li, Y.L. Ma, Extended generalized Darboux transformation to hybrid rogue wave and breather solutions for a nonlinear Schrödinger equation. Appl. Math. Comput. 386 (2020) 125469.

[36] Y.L. Ma, A.M. Wazwaz, B.Q. Li, New extended Kadomtsev–Petviashvili equation: multiple soliton solutions, breather, lump and interaction solutions, Nonlinear Dyn. Submitted.

[37] E.G. Fan, Auto-Backlund transformation and similarity reductions for general variable coefficient KdV equations, Phys. Lett. A 294 (2002) 26–30

[38] G.Q. Xu, Painlevé classiffication of a generalized coupled Hirota system, Phys. Rev. E 74 (2006) 027602.

[39] R. Hirota, The Direct Method in Soliton Theory, Cambridge University Press, Cambridge (2004)

[40] A.M. Wazwaz, The Hirota's direct method for multiple-soliton solutions for three model equations of shallow water waves, Appl. Math. Comput. 201 (2008) 489–503.

[41] B.Q. Li, Y.L. Ma, Interaction dynamics of hybrid solitons and breathers for extended generalization of Vakhnenko equation, Nonlinear Dyn. 102 (2020) 1787–1799.

[42] B.Q. Li, Loop-like kink breather and its transition phenomena for the Vakhnenko equation arising from high-frequency wave propagation in electromagnetic physics, Appl. Math. Lett. 112 (2021) 106822.

[43] Zhaqilao, Dynamics of localized wave solutions for the coupled Higgs field equation, Nonlinear Dyn. 101 (2020) 1181–1198.